Biochemistry and Biophysics Reports 26 (2021) 100968

Contents lists available at ScienceDirect

Biochemistry and Biophysics Reports

journal homepage: www.elsevier.com/locate/bbrep

Impaired neurite development and mitochondrial dysfunction associated with calcium accumulation in dopaminergic neurons differentiated from the dental pulp stem cells of a patient with metatropic dysplasia

Xiao Sun [a], Hiroki Kato [a], Hiroshi Sato [a], Michiko Torio [b], Xu Han [a], Yu Zhang [a], Yuta Hirofuji [a], Takahiro A. Kato [c], Yasunari Sakai [b], Shouichi Ohga [b], Satoshi Fukumoto [a,**], Keiji Masuda [a,*]

[a] Section of Oral Medicine for Children, Division of Oral Health, Growth and Development, Faculty of Dental Science, Kyushu University, Maidashi 3-1-1, Higashi-Ku, Fukuoka, 812-8582, Japan
[b] Department of Pediatrics, Graduate School of Medical Sciences, Kyushu University, Maidashi 3-1-1, Higashi-Ku, Fukuoka, 812-8582, Japan
[c] Department of Neuropsychiatry, Graduate School of Medical Sciences, Kyushu University, Maidashi 3-1-1, Higashi-Ku, Fukuoka, 812-8582, Japan

ARTICLE INFO

Keywords:
Dental pulp stem cells
Dopaminergic neuron
Metatropic dysplasia
Mitochondria
Reactive oxygen species
Transient receptor potential vanilloid 4

ABSTRACT

Transient receptor potential vanilloid member 4 (TRPV4) is a Ca^{2+} permeable nonselective cation channel, and mutations in the *TRPV4* gene cause congenital skeletal dysplasias and peripheral neuropathies. Although TRPV4 is widely expressed in the brain, few studies have assessed the pathogenesis of *TRPV4* mutations in the brain. We aimed to elucidate the pathological associations between a specific *TRPV4* mutation and neurodevelopmental defects using dopaminergic neurons (DNs) differentiated from dental pulp stem cells (DPSCs). DPSCs were isolated from a patient with metatropic dysplasia and multiple neuropsychiatric symptoms caused by a gain-of-function *TRPV4* mutation, c.1855C>T (p.L619F). The mutation was corrected by CRISPR/Cas9 to obtain isogenic control DPSCs. Mutant DPSCs differentiated into DNs without undergoing apoptosis; however, neurite development was significantly impaired in mutant vs. control DNs. Mutant DNs also showed accumulation of mitochondrial Ca^{2+} and reactive oxygen species, low adenosine triphosphate levels despite a high mitochondrial membrane potential, and lower peroxisome proliferator-activated receptor gamma coactivator 1-alpha expression and mitochondrial content. These results suggested that the persistent Ca^{2+} entry through the constitutively activated TRPV4 might perturb the adaptive coordination of multiple mitochondrial functions, including oxidative phosphorylation, redox control, and biogenesis, required for dopaminergic circuit development in the brain. Thus, certain mutations in *TRPV4* that are associated with skeletal dysplasia might have pathogenic effects on brain development, and mitochondria might be a potential therapeutic target to alleviate the neuropsychiatric symptoms of TRPV4-related diseases.

1. Introduction

Transient receptor potential vanilloid member 4 (TRPV4) is a Ca^{2+} permeable, nonselective cation channel that responds to multiple stimuli, including osmotic pressure, temperature, and mechanical stress [1]. Mutations in the gene encoding TRPV4 have been linked to both congenital skeletal dysplasias and neuropathies. Skeletal dysplasias are mainly characterized by a short trunk due to platyspondyly and scoliosis, and metatropic dysplasia (MD) is the most severe type [2]. Neuropathies include peripheral axonal neuropathies, that mainly affect motor neurons [3]. Numerous *TRPV4* mutations have been identified, many of which are gain-of-function mutations in the Ca^{2+} channel [1–3]. Although TRPV4-related skeletal dysplasias and neuropathies have been recognized as separate disorders, several reports have described patients with overlapping phenotypes [4–8].

Most previous studies have employed gene mutation analyses,

Abbreviations: ATP, adenosine triphosphate; DN, dopaminergic neuron; DPSC, dental pulp stem cell; MD, metatropic dysplasia; MPP, mitochondrial membrane potential; NURR1, nuclear receptor related 1; PGC-1α, peroxisome proliferator-activated receptor gamma coactivator 1-alpha; ROS, reactive oxygen species; RPL13A, 60S ribosomal protein L13a; SOD, superoxide dismutase; TRPV4, transient receptor potential vanilloid member 4.

* Corresponding author.
** Corresponding author.
E-mail addresses: fukumoto@dent.kyushu-u.ac.jp (S. Fukumoto), kemasuda@dent.kyushu-u.ac.jp (K. Masuda).

https://doi.org/10.1016/j.bbrep.2021.100968
Received 19 March 2020; Received in revised form 22 December 2020; Accepted 22 February 2021

clinical examinations using bone X-rays, nerve conduction studies, and Ca^{2+} permeability analyses in mutant *TRPV4*-transfected cell lines [3]. Studies using disease-specific models have shown that several mutations in *TRPV4* associated with skeletal dysplasia affect chondrogenic and osteogenic differentiation [9–13]. Although TRPV4 is widely expressed in the brain and is involved in various functions, few studies have focused on the pathological association between *TRPV4* mutations and neural cells [14,15]. A recent report described two siblings, both with peripheral neuropathy and severe intellectual disability caused by a *TRPV4* mutation [16]. Thus, certain mutations in *TRPV4* may affect different cell lineages, including those belonging to the skeletal, peripheral, and central nervous systems.

Human dental pulp stem cells (DPSCs) are mesenchymal stem cells that efficiently differentiate into different cell lineages, including osteoblasts, chondrocytes, and dopaminergic neurons (DNs) [17,18]. DNs are a neuronal subtype involved in multiple brain functions, including motor, reward, and cognitive functions [19]. Defects in DNs play important roles in many neuropsychiatric disorders including Parkinson's disease, schizophrenia and autism [19]. DPSCs derived from patients with neurodevelopmental disorders can be differentiated into DNs for analysis, as disease-specific cellular models [20–22]. Given that TRPV4 functions as a temperature-sensitive receptor involved in the excitability and Ca^{2+} homeostasis of DNs, this suggests that DNs may be affected by pathological mutations in *TRPV4* [23].

We aimed to elucidate the underlying mechanisms of neurodevelopmental defects associated with certain *TRPV4* mutations using DNs. To do this, DPSCs carrying a gain-of-function *TRPV4* mutation, c.1855C>T (p.L619F), were isolated from a patient with MD and neuropsychiatric symptoms [12,13]. The *TRPV4* mutation was corrected using genome editing to generate isogenic control cells. Mutant and control DPSCs were differentiated into DNs for examination.

2. Materials and methods

2.1. DPSC isolation and culture

Experiments using human samples were reviewed and approved by the Kyushu University Institutional Review Board for Human Genome/Gene Research (permission number: 678-02) and were conducted in accordance with the Declaration of Helsinki. Written informed consent was obtained from the patient's guardians.

DPSCs were isolated from a 14-year-old boy with MD carrying a de novo mutation in *TRPV4*, c.1855C>T (p.L619F) [12]. He had severe motor disabilities, hearing loss, and an intelligence quotient of 80. Brain magnetic resonance imaging did not identify any parenchymal lesions. At 12 years old, he developed epilepsy. Electroencephalograms revealed epileptiform discharges from the frontal and temporal lobes. The recurrent seizures were difficult to distinguish from somatoform disorders due to the patient's uncontrollable anxiety and other neuropsychiatric conditions.

The mutation was repaired by CRISPR/Cas9 to obtain isogenic control DPSCs (Ctrl-DNs) as previously described [12]. DPSCs were cultured in Alpha Modification of Eagle's Medium (Nacalai Tesque, Kyoto, Japan) containing 15% fetal bovine serum (Sigma-Aldrich, MO, USA), 100 μM L-ascorbic acid 2-phosphate (Wako Pure Chemical Industries, Osaka, Japan), 250 μg/mL fungizone (Thermo Fisher Scientific, MA, USA), 100 U/mL penicillin, and 100 μg/mL streptomycin (Nacalai Tesque) at 37°C and 5% CO_2. Cells passaged ≤7 times were used in all experiments.

2.2. DN differentiation of DPSCs

A total of 1×10^5 DPSCs were seeded onto a six-well plate and incubated overnight. Cells were then cultured in Dulbecco's Modified Eagle's Medium (Nacalai Tesque) supplemented with 20 ng/mL epidermal growth factor (Peprotech, NJ, USA), 20 ng/mL basic fibroblast growth factor (Peprotech), and 1% N2 supplement (Thermo Fisher Scientific) for 2 days. The medium was subsequently replaced with neurobasal media (Thermo Fisher Scientific) supplemented with 2% B27 supplement (Thermo Fisher Scientific), 1 mM dibutyryladenosine 3,5-cyclic monophosphate (Nacalai Tesque), 0.5 mM 3-isobutyl-1-methylxanthine (Sigma-Aldrich), and 200 μM ascorbic acid (Nacalai Tesque) and incubated for 5 days.

2.3. Immunocytochemistry and analysis of cultured DNs

DNs were cultured on cover glasses and fixed with 4% paraformaldehyde in 0.1 M sodium phosphate buffer (PBS, pH 7.4) for 10 min. Cells were subsequently permeabilized with 0.1% Triton X-100 for 5 min. Cells were blocked with 2% bovine serum albumin in phosphate-buffered saline for 20 min and then incubated with one of the following primary antibodies for 90 min: anti-TOMM20 (translocase of outer mitochondrial membrane 20) (Santa Cruz Biotechnology, CA, USA) or anti-tyrosine hydroxylase (TH; Proteintech, IL, USA). Cells were subsequently incubated with Alexa Fluor-conjugated secondary antibodies (Thermo Fisher Scientific). After staining with secondary antibodies in the dark for 60 min, nuclei were counterstained with 4′,6-diamidino-2-phenylindole (Dojindo, Kumamoto, Japan). The cover glass was then mounted on a slide using ProLong Diamond mounting medium (Thermo Fisher Scientific). Analysis of neurite outgrowth, branching, and the mitochondrial-stained area per cell area in the cultured DNs was performed as described previously [22].

2.4. Quantitative analysis of mitochondria in DNs

For the evaluation of mitochondrial content in DNs, TOMM20 was used as a specific mitochondrial marker, as described previously [20–22]. Fluorescence images of DNs stained with anti-TOMM20, anti-TH, and DAPI were acquired using a Nikon C2 confocal microscope (Nikon). The TOMM20-stained and TH-stained areas of each 30 cells randomly selected from the fluorescence images were measured as the mitochondrial and cell areas, respectively. Areas were measured using the Multi Wavelengths Cell Scoring module in the MetaMorph software (Molecular Devices, CA, USA). To normalize the content of mitochondria in whole cells, the TOMM20-stained areas were divided by TH-stained areas. To evaluate the localization of mitochondria in neurites, the number of neurites harboring at least one mitochondrion was counted and corrected with the total number of neurites in every 10 DNs randomly selected from the fluorescence images.

2.5. Measurement of mitochondrial membrane potential and intracellular adenosine triphosphate levels

Mitochondrial membrane potential (MMP) and intracellular adenosine triphosphate (ATP) levels were measured as described previously [21].

2.6. Measurement of mitochondrial reactive oxygen species levels

In order to measure mitochondrial reactive oxygen species (ROS) levels, the cells were cultured in μ-dishes (ibidi, Munich, Germany) and then incubated with 5 μM MitoSOX Red (Thermo Fisher Scientific) and 1 μM Mitotracker Green (Thermo Fisher Scientific) for 30 min at 37 °C. Fluorescent images of MitoSOX Red and Mitotracker Green signals were acquired using a Nikon C2 confocal microscope (Nikon). The fluorescence intensity of MitoSOX Red and Mitotracker Green were measured using the NIS-Elements software (Nikon). The intensity of MitoSOX Red was divided by that of Mitotracker Green to calculate mitochondrial ROS production per mitochondrion.

2.7. Intracellular and mitochondrial Ca^{2+} levels

Intracellular and mitochondrial Ca^{2+} levels were measured as described previously [24]. Briefly, cells were stained with Fluo-4 AM (to detect intracellular Ca^{2+}; Thermo Fisher Scientific) and Rhod-2 AM (to detect mitochondrial Ca^{2+}; Dojindo). Fluorescent signals were measured using an Infinite 200 PRO plate reader (Tecan, Männedorf, Switzerland). Fluorescent images were acquired using a Nikon C2 confocal microscope.

2.8. RNA extraction and quantitative real-time polymerase chain reaction (PCR)

Total RNA was extracted from cells using an RNeasy Mini Kit (Qiagen). First-strand cDNA was synthesized using the ReverTra Ace qPCR RT Master Mix with gDNA Remover (Toyobo, Osaka, Japan). The sequences of primers used were as follows: nuclear receptor related 1 (*NURR1*): 5′- GCACTTCGGCAGAGTTGAATGA-3′ (forward) and 5′-GGTGGCTGTGTTGCTGGTAGTT-3′ (reverse); peroxisome proliferator-activated receptor gamma coactivator 1-alpha (*PGC-1α*): 5′- GGCAGAAGGCAATTGAAGAG-3′ (forward) and 5′- TCAAAACGGTCCCTCAGTTC-3′ (reverse); superoxide dismutase 1 (*SOD1*): 5′-GGTGGGCCAAAGGATGAAGAG-3′ (forward) and 5′-CCACAAGCCAAACGACTTCC-3′ (reverse); superoxide dismutase 2 (*SOD2*): 5′-AAACCTCAGCCCTAACGGTG-3′ (forward) and 5′-GCCTGTTGTTCCTTGCAGTG-3′ (reverse); 60S ribosomal protein L13a (RPL13A): 5′-GCTGTGAAGGCATCAACATTT-3′ (forward) and 5′-CATCCGCTTTTTCTTGTCGTA-3′ (reverse). Real-time quantitative PCR was performed using the GoTaq qPCR Master Mix (Promega, WI, USA) and analyzed with the StepOnePlus Real-Time PCR System (Thermo Fisher Scientific). The relative expression levels of the target genes were analyzed using the comparative threshold cycle method by normalization against the levels of *RPL13A*.

2.9. Western blot analysis

TRPV4 protein levels were measured by western blotting as described previously [13].

2.10. Statistical analyses

Statistical analyses were performed by Student's *t*-test using JMP software version 14 (SAS Institute, NC, USA). Statistical significance was set at $P < 0.05$.

3. Results

3.1. Impaired neurite development of mutant DNs

Both mutant DPSCs and isogenic control DPSCs differentiated into DNs (Fig. 1A). No significant difference in *NURR1* expression, an essential factor for DN neurogenesis, was identified between the two groups (Fig. 1B). Approximately 80% of cultures in both groups expressed TH, the marker for mature DNs (Fig. 1C). However, the maximum neurite length was significantly shorter and the number of neurite branches was significantly lower in MD-DNs vs. Ctrl-DNs (Fig. 1D and E). These results suggested that patient-derived DPSCs with the p.L619F mutation could differentiate into DNs, but that neurite development was impaired.

3.2. Reduced mitochondrial content and cellular ATP levels in mutant DNs

Mitochondria play key roles in neurite elongation and branching.

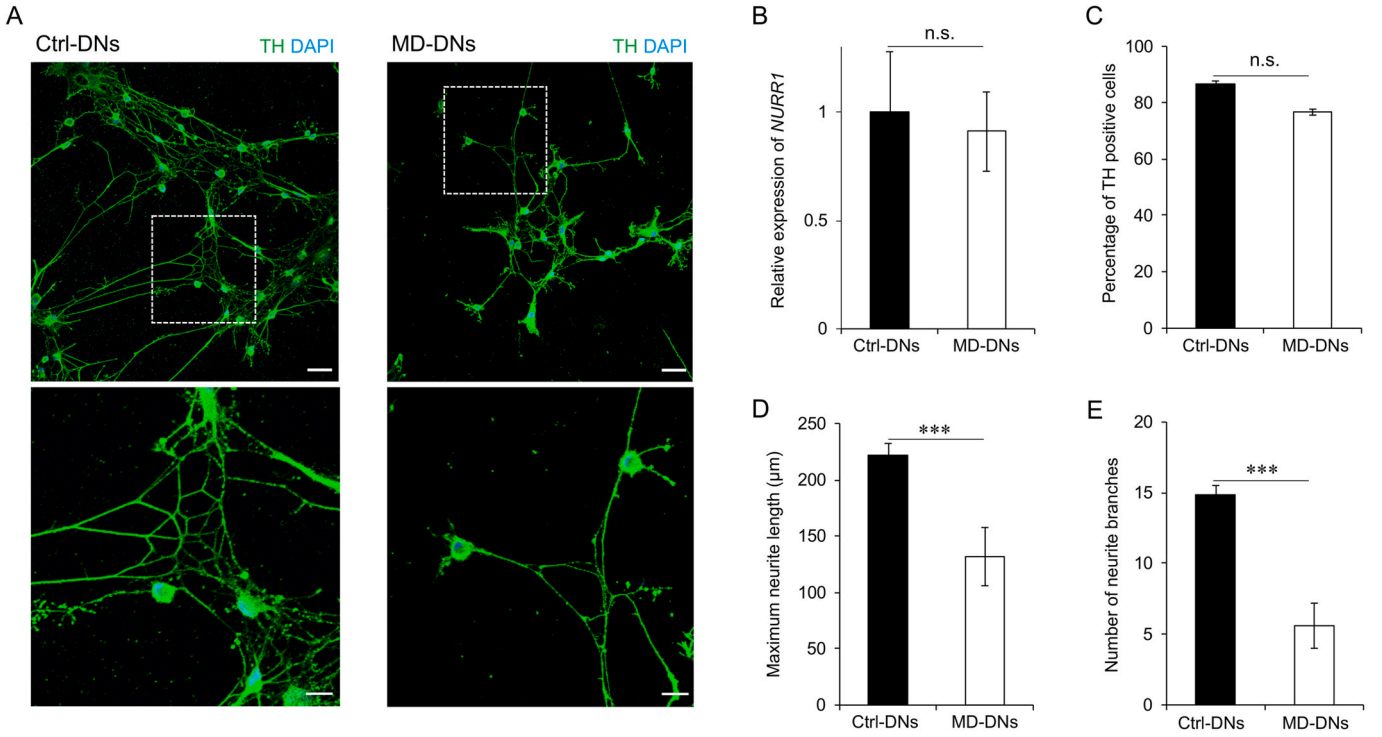

Fig. 1. Differentiation of dental pulp stem cells (DPSCs) into dopaminergic neurons (DNs). (A) DNs (control, Ctrl; MD, metatropic dysplasia) were visualized by immunofluorescence microscopy using anti-tyrosine hydroxylase (TH) antibodies. Nuclei were counterstained with 4′,6-diamidino-2-phenylindole (DAPI). Scale bars = 50 μm. The boxed regions are shown at greater magnification in the lower panels. Scale bars = 25 μm. (B) Nuclear receptor related 1 (*NURR1*) expression in DNs was measured using quantitative reverse transcription polymerase chain reaction. Means ± standard error of the means (SEMs) were obtained from three experiments. (C) The percentage of TH-positive cells was measured. (D, E) Maximum neurite length (D) and total number of branches per DN (E) were measured. (C–E) Means±SEMs were obtained after analyzing 30 cells from three experiments. n.s., not significant, ***$P < 0.001$.

The abundance and distribution of mitochondria in DNs were evaluated by immunostaining for TOMM20, which is localized in the mitochondrial outer membrane (Fig. 2A). Both the TOMM20-stained area per cell area and the proportion of neurites containing mitochondria were significantly lower in MD-DNs vs. Ctrl-DNs (Fig. 2B and C). MMP and ATP levels were measured to evaluate activity of mitochondrial oxidative phosphorylation. While the MMP was significantly higher (Fig. 2D and Supplementary Fig. S1), cellular ATP levels were significantly lower in MD-DNs vs. Ctrl-DNs (Fig. 2E). These results indicated dysregulated mitochondrial function in MD-DNs.

3.3. Increased intracellular and mitochondrial Ca^{2+} levels of mutant DNs

The p.L619F mutation is a gain-of-function mutation that increases the Ca^{2+} influx which accelerates chondrocyte and osteoblast differentiation [12,13]. Here, we found that both intracellular and mitochondrial Ca^{2+} levels were significantly higher in MD-DNs vs. Ctrl-DNs (Fig. 3A and B). TRPV4 expression levels were lower in MD-DPSCs vs. Ctrl-DPSCs, as previously reported [12,13] (Fig. 3C). TRPV4 expression was significantly higher after vs. before differentiation in both groups (Fig. 3C). After differentiation, TRPV4 expression was significantly higher in MD-DNs vs. Ctrl-DNs. These results suggested that the p.L619F mutation increased TRPV4 function and expression, which contributed to the higher Ca^{2+} levels observed in MD-DNs.

3.4. Increased mitochondrial ROS levels in mutant DNs

Increased mitochondrial Ca^{2+} stimulates mitochondrial respiration, which increases ROS production during the electron transport. The fluorescence intensity of MitoSOX-stained area/Mitotracker-stained area, which shows normalized mitochondrial ROS levels, was significantly higher in MD-DNs vs. Ctrl-DNs (Fig. 4A and B). The expression of *PGC-1α*, a master gene involved in mitochondrial biogenesis and closely related to ROS-mediated signaling, was significantly lower in MD-DNs vs. Ctrl-DNs (Fig. 4C). Additionally, the expression of *SOD2*, a downstream target of PGC-1α, was lower in MD-DNs vs. Ctrl-DNs, although *SOD1* expression was similar in both DNs (Fig. 4D and E).

We found no significant difference in the viable cell count after differentiation between the two groups and only a few apoptotic cells in both groups, as confirmed by the extremely low expression of truncated caspase-3 (Supplementary Fig. S2). These were consistent with the highly maintained MMP in MD-DNs, indicating that the mitochondrial

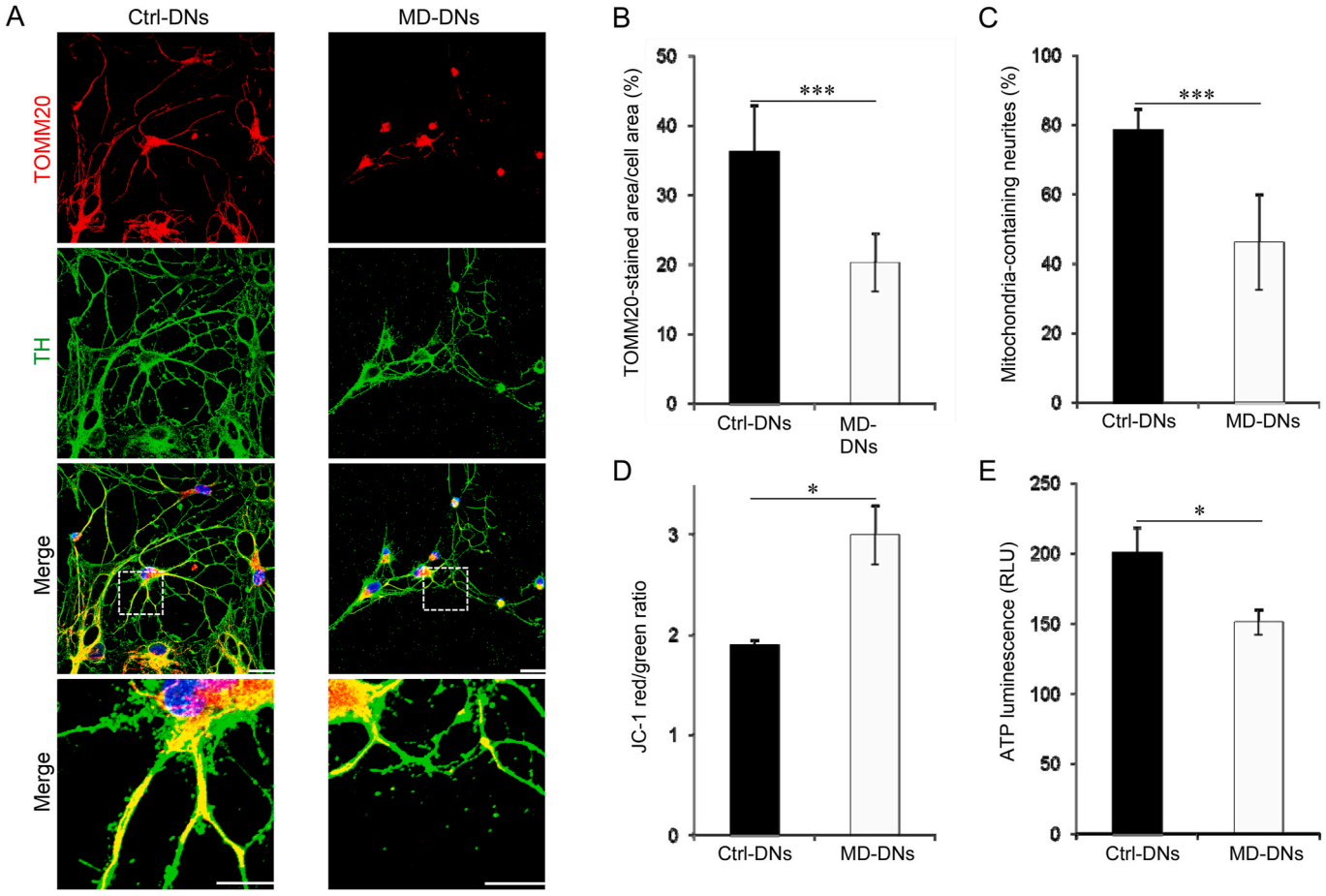

Fig. 2. Altered mitochondrial function of mutant (metatropic dysplasia, MD) vs. control (Ctrl) dopaminergic neurons (DNs). (A) DNs were stained with anti-TOMM20 (a mitochondrial marker) and anti-tyrosine hydroxylase (TH) antibodies and counterstained with 4′,6-diamidino-2-phenylindole. Scale bars = 25 μm. The boxed regions on the merged images are shown at greater magnification in the lower panels. Scale bars = 20 μm. (B) TOMM20-stained and cell area were measured using MetaMorph software. Then, TOMM20-stained areas were divided by cell areas. Three independent experiments ware performed. Means ± standard error of the means (SEMs) were obtained after analyzing each 30 cells from three independent experiments. (C) The percentage of mitochondria-containing neurites is shown. The number of neurite with at least one mitochondrion was divided by the total number of neurites to normalize the ratio of mitochondria-containing neurites between the two groups with differential neurite development. Three independent experiments were performed. Means±SEMs were obtained after analyzing each 10 cells from three independent experiments. (D) Mitochondrial membrane potential was measured by JC-1. The ratio of JC-1 red/green was calculated. (E) The adenosine triphosphate (ATP) levels were measured by luminescence assay. The ATP luminescence signals were divided by the number of cells. (D, E) Means±SEMs were obtained from three experiments. *P < 0.05, ***P < 0.001. (For interpretation of the references to colour in this figure legend, the reader is referred to the Web version of this article.)

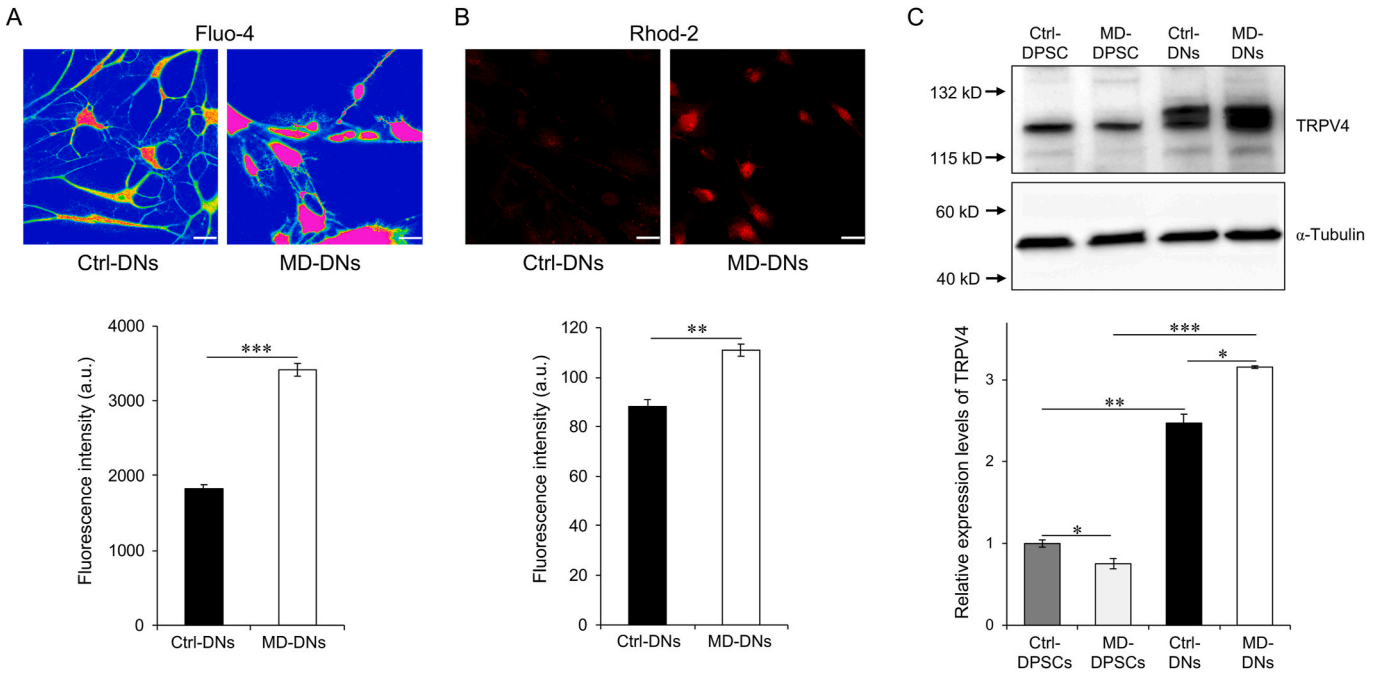

Fig. 3. Enhanced intracellular and mitochondrial Ca^{2+} levels in mutant (metatropic dysplasia, MD) vs. control (Ctrl) dopaminergic neurons (DNs). (A) Cells were stained with Fluo-4 AM and observed by immunofluorescence microscopy, and the fluorescence intensity of Fluo-4 AM was measured using a plate reader. (B) Cells were stained with Rhod-2 AM and observed by immunofluorescence microscopy, and the fluorescence intensity of Rhod-2 AM was measured using a plate reader. Scale bars = 25 μm. (C) Transient receptor potential vanilloid member 4 (TRPV4) expression in dental pulp stem cells (DPSCs) and DNs was measured by western blotting. TRPV4 expression was normalized to α-tubulin. Means ± standard error of the means were obtained from three experiments. *P < 0.05, **P < 0.01, ***P < 0.001.

membrane was intact (Fig. 2D).

Together, these results suggested that in MD-DNs, mitochondrial ROS levels were deleterious enough to downregulate *PGC-1α* and *SOD2*, but not to trigger apoptosis.

4. Discussion

Herein, DPSCs carrying the *TRPV4* p.L619F mutation differentiated into DNs without undergoing apoptosis, but neurite development was impaired compared to isogenic control cells. Mutant DNs also showed reduced ATP levels, *PGC-1α* expression, and mitochondrial content, but elevated MMP, mitochondrial Ca^{2+}, and ROS levels. These results imply that Ca^{2+} accumulation through an MD-related gain-of-function mutation in *TRPV4*, c.1855C>T (p.L619F) might dysregulate the mitochondrial function required for the post-differentiation development of DNs.

Mitochondrial function is tightly regulated by Ca^{2+} [25–27]. In physiological conditions, increased mitochondrial Ca^{2+} activates oxidative phosphorylation, including enzymes involved in the Krebs cycle and respiratory chain complexes. This accelerates electron transport to elevate the MMP and ATP synthesis. However, persistent mitochondrial Ca^{2+} overload induces mitochondrial membrane depolarization, permeability transition, and finally cell death [27]. In MD-DNs, we observed high mitochondrial Ca^{2+}, MMP, and ROS levels, suggesting that increased mitochondrial Ca^{2+} activated electron flow to elevate the MMP, which might have triggered excessive ROS generation through electron leakage. However, most MD-DNs survived without undergoing apoptosis, indicating an intact mitochondrial membrane. Thus, in MD-DNs, the increased mitochondrial Ca^{2+} induced by TRPV4 with the p.L619F mutation might have both positive and negative effects that collectively perturb mitochondrial function.

ROS play essential roles in mitochondrial biogenesis [28,29]. Given the elevated ROS levels and reduced mitochondrial content and *PGC-1α* expression we observed in MD-DNs, the low cellular ATP levels despite a high MMP might correlate with the reduced ROS-regulated mitochondrial biogenesis in these cells. In mammals, mitochondrial biogenesis is positively or negatively regulated, depending on the type of stress induced, leading to the hypothesis that acute or moderate oxidative stress adaptively induces PGC-1α-mediated mitochondrial biogenesis, whereas prolonged or extensive stress induces the opposite outcome [29–35]. In MD-DNs, excessive ROS generated through persistently accelerated electron flow by Ca^{2+} accumulation might inhibit *PGC-1α* induction and mitochondrial biogenesis during neurite development. Downregulation of *SOD2*, a target of PGC-1α, might also be involved in mitochondrial ROS accumulation [31].

Mitochondrial dysfunction have not yet fully explained the MD-related neuropsychiatric pathology in our case, because only a few neurological defects have been reported to be associated with the pathophysiology of MD. However, autism and other polygenic neuropsychiatric disorders have provided evidence for the pathogenic effects of mitochondrial respiration, biogenesis, morphology, redox control and Ca^{2+} regulation on their phenotypic expression [36]. On the other hand, a calcium channel-associated disorder Timothy syndrome, exhibits prominent neurodevelopmental features of autism, intellectual disability and seizures [37]. Given the critical association of mitochondrial functions with intracellular Ca^{2+} signaling pathways, genetic variants in TRPV4 may be risk factors for impairing mitochondrial function in polygenic neuropsychiatric phenotypes [37].

This study has several limitations in terms of understanding the pathology of neuropsychiatric symptoms in TRPV4-related skeletal dysplasias. Impaired DN development might contribute to the psychogenic seizures that are associated with anxiety and/or mild intellectual disability. However, it remains to be determined whether overlapping molecular signals are involved in the pathogenesis of the severe skeletal and cognitive development impairments that occur in patients with MD. Further studies are required to elucidate the precise mechanisms underlying the neuropsychiatric phenotypes and brain development that are associated with *TRPV4* mutations, including careful examinations of patients' neuropsychiatric symptoms and altered brain dopaminergic

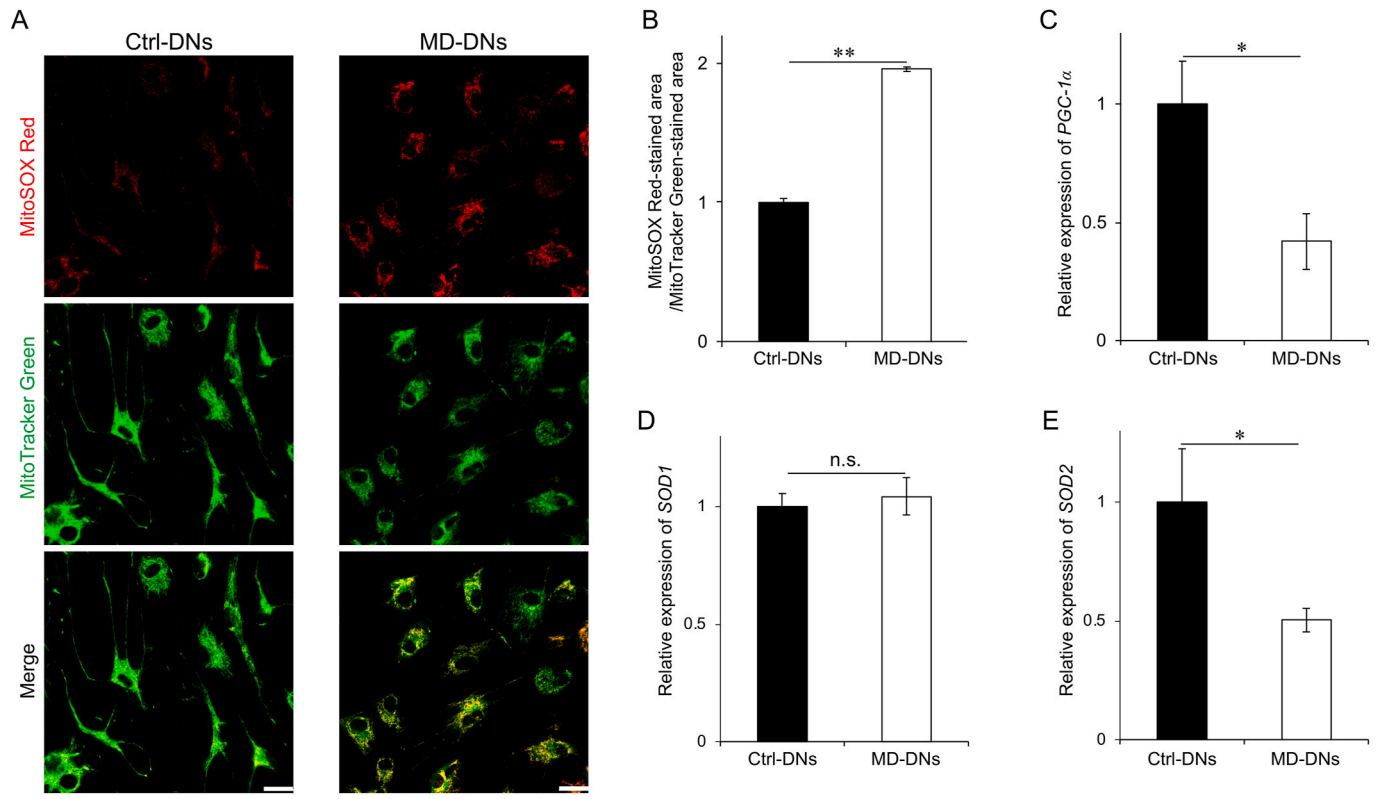

Fig. 4. Elevated mitochondrial reactive oxygen species (ROS) levels in mutant (metatropic dysplasia, MD) vs. control (Ctrl) dopaminergic neurons (DNs). (A) DNs were stained with MitoSOX Red (a mitochondrial ROS indicator) and MitoTracker Green (a mitochondrial marker). Scale bars = 25 μm. (B) To measure the ROS level per mitochondrion, the fluorescence intensity of MitoSOX Red was divided by that of MitoTracker Green. (C–E) Peroxisome proliferator-activated receptor gamma coactivator 1-alpha (*PGC-1α*), and superoxide dismutase 1 and 2 (*SOD1* and *SOD2*) mRNA expression in DNs was measured using quantitative reverse transcription polymerase chain reaction. (B–E) Means ± standard error of the means were obtained from three experiments. n.s., not significant, *P < 0.05, **P < 0.01. (For interpretation of the references to colour in this figure legend, the reader is referred to the Web version of this article.)

signaling, along with assessments of the ROS-mediated signaling pathways leading to *PGC-1α* downregulation, endoplasmic reticulum and reactive nitrogen species as alternative pathological elements, the potential effects on excitatory or inhibitory neurons, and regulation of TRPV4 expression during neural differentiation.

In conclusion, persistent Ca^{2+} accumulation through a *TRPV4* gain-of-function mutation perturbs coordination between mitochondrial respiration, redox control, and biogenesis during DN development. These findings suggest that certain *TRPV4* mutations have pathogenic effects on both the bone and central nervous system. Mitochondrial activation, and mitochondrial biogenesis and antioxidant capacity enhancement, might be potential therapeutic targets for alleviating neuropsychiatric symptoms in TRPV4-related diseases.

Disclosure

Dr. Sun has nothing to disclose.

Dr. Hiroki Kato reports grants from KAKENHI JP19K10406, during the conduct of the study;.

Dr. Sato has nothing to disclose.

Dr. Torio has nothing to disclose.

Dr. Han has nothing to disclose.

Dr. Zhang has nothing to disclose.

Dr. Hirofuji has nothing to disclose.

Dr. Takahiro A. Kato has nothing to disclose.

Dr. Sakai has nothing to disclose.

Dr. Ohga has nothing to disclose.

Dr. Fukumoto has nothing to disclose.

Dr. Masuda reports grants from KAKENHI JP19K10387, during the conduct of the study;.

Authorship contribution statement

Xiao Sun and Hiroki Kato: Conceptualization, Investigation, Formal analysis, Methodology, Writing - Original Draft, Writing - Review & Editing, Final approval of the version to be published. Hiroshi Sato, Xu Han, Yu Zhang, and Yuta Hirofuji: Methodology, Resources, Final approval of the version to be published. Michiko Torio, Takahiro A. Kato, Yasunari Sakai, and Shouichi Ohga: Validation, Writing - Original Draft, Writing - Review & Editing, Final approval of the version to be published. Satoshi Fukumoto and Keiji Masuda: Conceptualization, Methodology, Writing - Original Draft, Writing - Review & Editing, Project administration, Final approval of the version to be published.

Declaration of competing interest

All authors declare no conflicts of interest.

Acknowledgements

We thank the members of the Department of Pediatric Dentistry and Special Needs Dentistry at Kyushu University Hospital for their valuable suggestions, technical support, and materials. We appreciate the technical assistance that was provided by the Research Support Center at the Research Center for Human Disease Modeling, Kyushu University Graduate School of Medical Sciences. This work was supported by the Japan Society for the Promotion of Science [KAKENHI; grant numbers, JP19K10387 and JP19K10406].

Appendix A. Supplementary data

Supplementary data to this article can be found online at https://doi.org/10.1016/j.bbrep.2021.100968.

References

[1] B. Nilius, T. Voets, The puzzle of TRPV4 channelopathies, EMBO Rep. 14 (2013) 152–163.

[2] G. Nishimura, E. Lausch, R. Savarirayan, M. Shiba, J. Spranger, B. Zabel, S. Ikegawa, A. Superti-Furga, S. Unger, TRPV4-associated skeletal dysplasias, Am J Med Genet C Semin Med Genet 160C (2012) 190–204.

[3] M. McEntagart, TRPV4 axonal neuropathy spectrum disorder, J. Clin. Neurosci. 19 (2012) 927–933.

[4] M. Zimoń, J. Baets, M. Auer-Grumbach, J. Berciano, A. Garcia, E. Lopez-Laso, L. Merlini, D. Hilton-Jones, M. McEntagart, A.H. Crosby, N. Barisic, E. Boltshauser, C.E. Shaw, G. Landouré, C.L. Ludlow, R. Gaudet, H. Houlden, M.M. Reilly, K. H. Fischbeck, C.J. Sumner, V. Timmerman, A. Jordanova, P.D. Jonghe, Dominant mutations in the cation channel gene transient receptor potential vanilloid 4 cause an unusual spectrum of neuropathies, Brain 133 (2010) 1798–1809.

[5] D.H. Chen, Y. Sul, M. Weiss, A. Hillel, H. Lipe, J. Wolff, M. Matsushita, W. Raskind, T. Bird, CMT2C with vocal cord paresis associated with short stature and mutations in the TRPV4 gene, Neurology 75 (2010) 1968–1975.

[6] S. Unger, E. Lausch, F. Stanzial, G. Gillessen-Kaesbach, I. Stefanova, C.M. Di Stefano, E. Bertini, C. Dionisi-Vici, B. Nilius, B. Zabel, A. Superti-Furga, Fetal akinesia in metatropic dysplasia: the combined phenotype of chondrodysplasia and neuropathy? Am. J. Med. Genet. 155A (2011) 2860–2864.

[7] T.J. Cho, K. Matsumoto, V. Fano, J. Dai, O.H. Kim, J.H. Chae, W.J. Yoo, Y. Tanaka, Y. Matsui, I. Takigami, S. Monges, B. Zabel, K. Shimizu, G. Nishimura, E. Lausch, S. Ikegawa, TRPV4-pathy manifesting both skeletal dysplasia and peripheral neuropathy: a report of three patients, Am. J. Med. Genet. 158A (2012) 795–802.

[8] E. Faye, P. Modaff, R. Pauli, J. Legare, Combined phenotypes of spondylometaphyseal dysplasia-kozlowski type and charcot-marie-tooth disease type 2C secondary to a TRPV4 pathogenic variant, Mol Syndromol 10 (2019) 154–160.

[9] M.M. Weinstein, S.W. Tompson, Y. Chen, B. Lee, D.H. Cohn, Mice expressing mutant Trpv4 recapitulate the human TRPV4 disorders, J. Bone Miner. Res. 29 (2014) 1815–1822.

[10] B. Saitta, J. Passarini, D. Sareen, L. Ornelas, A. Sahabian, S. Argade, D. Krakow, D. H. Cohn, C.N. Svendsen, D.L. Rimoin, Patient-derived skeletal dysplasia induced pluripotent stem cells display abnormal chondrogenic marker expression and regulation by BMP2 and TGFβ1, Stem Cell. Dev. 23 (2014) 1464–1478.

[11] L. Hurd, S.M. Kirwin, M. Boggs, W.G. Mackenzie, M.B. Bober, V.L. Funanage, R. L. Duncan, A mutation in TRPV4 results in altered chondrocyte calcium signaling in severe metatropic dysplasia, Am. J. Med. Genet. 167A (2015) 2286–2293.

[12] K. Nonaka, X. Han, H. Kato, H. Sato, H. Yamaza, Y. Hirofuji, K. Masuda, Novel gain-of-function mutation of *TRPV4* associated with accelerated chondrogenic differentiation of dental pulp stem cells derived from a patient with metatropic dysplasia, Biochem Biophys Rep 19 (2019) 100648.

[13] X. Han, H. Kato, H. Sato, Y. Hirofuji, S. Fukumoto, K. Masuda, Accelerated osteoblastic differentiation in patient-derived dental pulp stem cells carrying a gain-of-function mutation of TRPV4 associated with metatropic dysplasia, Biochem. Biophys. Res. Commun. 523 (2020) 841–846.

[14] P. Kanju, W. Liedtke, Pleiotropic function of TRPV4 ion channels in the central nervous system, Exp. Physiol. 101 (2016) 1472–1476.

[15] H. Kumar, S.H. Lee, K.T. Kim, X. Zeng, I. Han, TRPV4: a sensor for homeostasis and pathological events in the CNS, Mol. Neurobiol. 55 (2018) 8695–8708.

[16] M.L. Thibodeau, C.H. Peters, K.N. Townsend, Y. Shen, G. Hendson, S. Adam, K. Selby, P.M. Macleod, C. Gershome, P. Ruben, S.J.M. Jones, the Forge Canada Consortium, J.M. Friedman, W.T. Gibson, G.A. Horvath, Compound heterozygous TRPV4 mutations in two siblings with a complex phenotype including severe intellectual disability and neuropathy, Am. J. Med. Genet. 173A (2017) 3087–3092.

[17] M. Kanafi, D. Majumdar, R. Bhonde, P. Gupta, I. Datta, Midbrain cues dictate differentiation of human dental pulp stem cells towards functional dopaminergic neurons, J. Cell. Physiol. 229 (2014) 1369–1377.

[18] H. Fujii, K. Matsubara, K. Sakai, M. Ito, K. Ohno, M. Ueda, A. Yamamoto, Dopaminergic differentiation of stem cells from human deciduous teeth and their therapeutic benefits for Parkinsonian rats, Brain Res. 1613 (2015) 59–72.

[19] M.O. Klein, D.S. Battagello, A.R. Cardoso, D.N. Hauser, J.C. Bittencourt, R. G. Correa, Dopamine: functions, signaling, and association with neurological diseases, Cell. Mol. Neurobiol. 39 (2019) 31–59.

[20] S. Hirofuji, Y. Hirofuji, H. Kato, K. Masuda, H. Yamaza, H. Sato, F. Takayama, M. Torio, Y. Sakai, S. Ohga, T. Taguchi, K. Nonaka, Mitochondrial dysfunction in dopaminergic neurons differentiated from exfoliated deciduous tooth-derived pulp stem cells of a child with Rett syndrome, Biochem. Biophys. Res. Commun. 498 (2018) 898–904.

[21] H.T.N. Nguyen, H. Kato, K. Masuda, H. Yamaza, Y. Hirofuji, H. Sato, T.T.M. Pham, F. Takayama, Y. Sakai, S. Ohga, T. Taguchi, K. Nonaka, Impaired neurite development associated with mitochondrial dysfunction in dopaminergic neurons differentiated from exfoliated deciduous tooth-derived pulp stem cells of children with autism spectrum disorder, Biochem Biophys Rep 16 (2018) 24–31.

[22] H.T.N. Nguyen, H. Kato, H. Sato, H. Yamaza, Y. Sakai, S. Ohga, K. Nonaka, K. Masuda, Positive effect of exogenous brain-derived neurotrophic factor on impaired neurite development and mitochondrial function in dopaminergic neurons derived from dental pulp stem cells from children with attention deficit hyperactivity disorder, Biochem. Biophys. Res. Commun. 513 (2019) 1048–1054.

[23] E. Guatteo, K.K. Chung, T.K. Bowala, G. Bernardi, N.B. Mercuri, J. Lipski, Temperature sensitivity of dopaminergic neurons of the substantia nigra pars compacta: involvement of transient receptor potential channels, J. Neurophysiol. 94 (2005) 3069–3080.

[24] H. Kato H, X. Han, H. Yamaza, K. Masuda, Y. Hirofuji, H. Sato, T.T.M. Pham, T. Taguchi, K. Nonaka, Direct effects of mitochondrial dysfunction on poor bone health in Leigh syndrome, Biochem. Biophys. Res. Commun. 493 (2017) 207–212.

[25] P.S. Brookes, Y. Yoon, J.L. Robotham, M.W. Anders, S.S. Sheu, Calcium, ATP, and ROS: a mitochondrial love-hate triangle, Am. J. Physiol. Cell Physiol. 287 (2004) C817–C833.

[26] R.M. Denton, Regulation of mitochondrial dehydrogenases by calcium ions, Biochim. Biophys. Acta 1787 (2009) 1309–1316.

[27] B. Glancy, R.S. Balaban, Role of mitochondrial Ca^{2+} in the regulation of cellular energetics, Biochemistry 51 (2012) 2959–2973.

[28] A. Thirupathi, C.T. de Souza, Multi-regulatory network of ROS: the interconnection of ROS, PGC-1 alpha, and AMPK-SIRT1 during exercise, J. Physiol. Biochem. 73 (2017) 487–494.

[29] C. Bouchez, A. Devin, Mitochondrial biogenesis and mitochondrial reactive oxygen species (ROS): a complex relationship regulated by the cAMP/PKA signaling pathway, Cells 8 (2019), https://doi.org/10.3390/cells8040287.

[30] A. Garnier, D. Fortin, C. Deloménie, I. Momken, V. Veksler, R. Ventura-Clapier, Depressed mitochondrial transcription factors and oxidative capacity in rat failing cardiac and skeletal muscles, J. Physiol. 551 (2003) 491–501.

[31] J. St-Pierre, S. Drori, M. Uldry, J.M. Silvaggi, J. Rhee, S. Jäger, C. Handschin, K. Zheng, J. Lin, W. Yang, D.K. Simon, R. Bachoo, B.M. Spiegelman, Suppression of reactive oxygen species and neurodegeneration by the PGC-1 transcriptional coactivators, Cell 127 (2006) 397–408.

[32] S. Javadov, D.M. Purdham, A. Zeidan, M. Karmazyn, NHE-1 inhibition improves cardiac mitochondrial function through regulation of mitochondrial biogenesis during postinfarction remodeling, Am. J. Physiol. Heart Circ. Physiol. 291 (2006) H1722–H1730.

[33] B. Wang, J. Sun, Y. Ma, G. Wu, Y. Tian, Y. Shi, G. Le, Resveratrol preserves mitochondrial function, stimulates mitochondrial biogenesis, and attenuates oxidative stress in regulatory T cells of mice fed a high-fat diet, J. Food Sci. 79 (2014) H1823–H1831.

[34] S. Baldelli, K. Aquilano, M.R. Ciriolo, PGC-1α buffers ROS-mediated removal of mitochondria during myogenesis, Cell Death Dis. 5 (2014) e1515.

[35] W.C. Lee, L.C. Li, J.B. Chen, H.W. Chang, Indoxyl sulfate-induced oxidative stress, mitochondrial dysfunction, and impaired biogenesis are partly protected by vitamin C and N-acetylcysteine, Sci. World J. 2015 (2015) 620826.

[36] V. Rangaraju, T.L. Lewis Jr., Y. Hirabayashi, M. Bergami, E. Motori, R. Cartoni, S. K. Kwon, J. Courchet, Pleiotropic mitochondria: the influence of mitochondria on neuronal development and disease, J. Neurosci. 39 (2019) 8200–8208.

[37] J.J. Gargus, Genetic calcium signaling abnormalities in the central nervous system: seizures, migraine, and autism, Ann. N. Y. Acad. Sci. 1151 (2009) 133–156.